NUMERICAL INVESTIGATION OF HYDROGEN-AIR DEFLAGRATIONS IN A REPEATED PIPE CONGESTION

Vendra C. Madhav Rao[1], Pratap Sathiah[2] and Jennifer X. Wen[1]
[1]Warwick FIRE, School of Engineering, University of Warwick, Coventry, CV4 7AL, UK, jennifer.wen@warwick.ac.uk
[2]Shell Technology Centre Bangalore, Shell India Markets Private Limited, Plot No - 7, Bangalore Hardware Park, Devanahalli, Mahadeva Kodigehalli, Bangalore, 562 149, Karnataka, India, pratap.sathiah@shell.com.

ABSTRACT

Emerging hydrogen energy technologies are creating new avenues for bring hydrogen fuel usage into larger public domain. Identification of possible accidental scenarios and measures to mitigate associated hazards should be well understood for establishing best practice guidelines. Accidentally released hydrogen forms flammable mixtures in a very short time. Ignition of such a mixture in congestion and confinements can lead to greater magnitudes of overpressure, catastrophic for both structure and people around. Hence understanding of the permissible level of confinements and congestion around the hydrogen fuel handling and storage unit is essential for process safety. In the present study, numerical simulations have been performed for the hydrogen-air turbulent deflagration in a well-defined congestion of repeated pipe rig, experimentally studied by [1]. Large Eddy Simulations (LES) have been performed using the in-house modified version of the OpenFOAM code. The Flame Surface Wrinkling Model in the LES context is used for modelling deflagrations. Numerical predictions concerning the effects of hydrogen concentration and congestion on turbulent deflagration overpressure are compared with the measurements [1] to provide validation of the code. Further insight about the flame propagation and trends of the generated overpressures over the range of concentrations are discussed.

1.0 INTRODUCTION

Hydrogen can play important role in reducing the greenhouse gas emissions from the usage of fossil fuels. Hydrogen as energy carrier applications are steadily on increase in automotive and portable power generation units based on fuel cell technologies. Due to Hydrogens low minimum ignition energy, high diffusivity and wide flammability limits, any accidental process leakages with subsequent ignition can lead to explosion i.e. rapid combustion, releasing heat, hot combustion products and shock waves. The hydrogen processes either at generation, storage and distribution are associated with the compressor, pumps or other auxiliary units, hence be it at the storage or at the usage site often it is associated with some level of congestion. The congestion present at the site can further extend the accidental explosion hazards region. Hydrogen is relatively new in public domain as fuel, identifying the risks associated with these kind of applications are very essential for process design and safe operation of the hydrogen installations. Also well identified risk can lead to establishment of new codes and safety standards for hydrogen. The experimental campaign to understand the potential and level of hazards associated with hydrogen installations was led by Shell Hydrogen B.V. and was co-funded by BP Gas Marketing Limited, ExxonMobil Research and Engineering Company and the U.K. Health and Safety Executive. The experimental campaign were carried out in three phases. In the first phase, experiments were conducted to establish hydrogen-air explosion overpressures magnitudes in a well-defined and well understood repeated pipe congestion geometries [1]. For the second and third phases of the experimental campaign, more realistic environments were chosen; a stack of dummy storage cylinders representing the high-pressure hydrogen storage [3] and a dummy vehicle and dispenser units in a mock refuelling station [4].

Numerical simulations have been performed mimicking these experimental conditions by various research groups to develop more reliable modelling approach and to fill in the experimental knowledge gaps. CFD simulations of homogenous hydrogen air mixture explosion in a mock-up refuelling station environment based on the experimental setup of [3] were conducted by [5,6,7,8,9,10]. The predictions of various CFD codes were compared with each other and with the experimental data.

The concentration distribution due to hydrogen leakage in a refuelling station by means of CFD were established. The effect of wind direction and ignition source on dispersion and explosion of hydrogen flammable cloud were also investigated in the experimental setup of [1]. The CFD simulations of turbulent deflagration in premixed hydrogen-air cloud in a mock hydrogen cylinder storage congestion were studied by [11] based on the experimental set up of [3]. The effects of ignition location, congestion and confining walls on the turbulent deflagrations in particular on explosion overpressure are discussed in details. These numerical studies have provided insight and complimented the experimental findings of the possible overpressure magnitudes in worst case scenarios to environmental vagary conditions, which are difficult to maintain in such large scale outdoor experiments.

In the present study, numerical simulations have been performed for hydrogen-air turbulent deflagration in the well-defined congestion of repeated pipe rig, experimentally studied by [1]. The simulations are performed using open-source OpenFOAM solver. The remaining paper is structured as follows. The CFD and combustion model used is described in Section 2. In particular, the governing equations for combustion model (i.e. regress variable and flame surface density) are presented in detail. The following sections 3 and 4 describe the experimental setup and numerical settings used in our simulations. Section 5, presents results of the validation work and CFD predictions. Finally, summary and conclusions are presented in Section 6.

2.0 NUMERICAL MODELLING

The governing Navier-Stokes equations are numerically solved in explicit Large Eddy Simulation (LES) method. The one equation eddy viscosity model, which solves a transport equation for the subgrid scale turbulent kinetic energy, is used for evaluating the sub-grid scale viscosity [12]. The Flame Surface Wrinkling Model developed by [13] is adopted for simulating the turbulent deflagrations. The governing equations are solved sequentially with iterations over the explicit coupling terms to obtain convergence. The segregate approach results in a courant number restriction [12]. Courant number of 0.1 was used in the present numerical simulations.

2.1 Combustion modelling

The Flame Surface Wrinkling Model is based on the laminar flamelet concept, uses conditional filtering to create a set of transport equations representing the flame front propagation process [13,14]. The flamelet concept simplifies the turbulent combustion treatment as it separates the combustion modelling from the analysis of the turbulent flow field by assuming that reaction takes place in relatively thin layers that separate regions of unburned and fully burned gases. The unburnt zone volume fraction is denoted as regress variable (b), taking values b = 1 in fresh gases and b = 0 in fully burnt gas region. The transport equation for the resolved part of regress variable is given as:

$$\frac{\partial \overline{\rho}\tilde{b}}{\partial t} + \nabla.\left(\overline{\rho}\tilde{U}\tilde{b}\right) - \nabla.\left(\overline{\rho}\mu_{sgs}\nabla\tilde{b}\right) = -\overline{\rho_u} S_L \Xi \left|\nabla\tilde{b}\right| \tag{1}$$

where, Ξ is subgrid flame wrinkling, can be regarded as the turbulent to laminar flame speed ratio and is formally related to the flame surface density by $\sum = \Xi |\nabla \overline{b}|$, ρ is the density, S_L is laminar flame speed and μ_{sgs} is the subgrid turbulent diffusion coefficient. Symbols ($\overline{\ }$) and ($\tilde{\ }$) represent the filtered and the density weighted filtering operations respectively. The subscripts u indicates conditioning on the unburned gases region. The resolved unburned gas volume fraction $\overline{b}$ is related to $\tilde{b}$ through $\overline{\rho}_u \overline{b} = \overline{\rho}\tilde{b}$. The closure for the sub-grid wrinkling is provided by a balanced transport equation,

$$\frac{\partial \overline{\rho}\Xi}{\partial t} + \hat{U}_s.\nabla\Xi = \overline{\rho} G \Xi - \overline{\rho} R(\Xi - 1) + \overline{\rho}\max\left[\left(\sigma_s - \sigma_t\right), 0\right]\Xi \tag{2}$$

where, $\hat{U}_s$ is the surface filtered local instantaneous velocity of the flame, which is modelled as

$$\widehat{U}_s = \tilde{U} + (\frac{\bar{\rho}_u}{\bar{\rho}} - 1) S_L \Xi n_f - \frac{\nabla.(\bar{\rho}\,\mu_{sgs} \nabla \tilde{b})}{\bar{\rho}\,|\nabla \tilde{b}|} n_f \tag{3}$$

The direction of flame propagation is $n_f = \nabla\tilde{b} / |\nabla\tilde{b}|$, σ_S and σ_t are the surface filtered resolved strain-rates relating to the surface filtered local instantaneous velocity of the flame ($\widehat{U}_s$) and surface filtered effective flame velocity of the flame surface ($\widehat{U}_t$), modelled as

$$\sigma_t = \nabla.(\tilde{U} + S_L \Xi\, n_f) - n_f.[\nabla(\tilde{U} + S_L \Xi n_f)].n_f$$

$$\sigma_s = \frac{\nabla\tilde{U} - n_f\,(\nabla\tilde{U})\,n_f}{\Xi} + \frac{(\Xi+1)[\nabla\,(S_L\, n_f) - n_f[\nabla(S_L\, n_f)\, n_f]}{2\Xi} \tag{4}$$

The terms $G\Xi$ and $R(\Xi - 1)$ in Eq. 2 are sub-grid turbulence generation and removal rate, with G and R as rate coefficients requiring modelling. The modelling of these terms is based on flame-speed correlation of [15] are given below

$$G = R\frac{\Xi_{eq} - 1}{\Xi_{eq}} \quad \text{and} \quad R = \frac{0.28}{\tau_\eta}\frac{\Xi^*_{eq}}{\Xi^*_{eq} - 1}\,,$$

$$\Xi^*_{eq} = 0.7\left(\frac{\hat{u}}{S_L}\right)^{\frac{1}{2}} (\Delta/\delta)^{1/6} Le^{-n} \text{ and } \Xi_{eq} = 1 + 2(1-b)(\Xi^*_{eq} - 1) \tag{5}$$

where, τ_n is the Kolmogorov time scale, $\hat{u}$ is the sub grid turbulence intensity and Le is the Lewis number, Δ is filter size and δ is laminar flame thickness. The unstrained laminar flame speed for hydrogen-air mixture is adopted from [16], this correlation is valid for mixture with equivalence ratio between 0.5 to 5.0.

3.0 EXPERIMENT DETAILS

The pipe rig comprises of a 3 m (width) x 3 m (depth) x 2 m (height) metal frame structure as shown in Figure 1. It consists of eighteen 1 m^3 cubic units i.e. 9 cubes in bottom layer and 9 in top layer. The framework is designed to hold metal grids. For the nominal 20 % area congestion, each grid comprised of several 26 ± 1 mm diameter bars spaced at 125 mm apart.

Figure 1. Experimental pipe rig setup with 4-gate configuration [1]

The gates are inserted vertically into the lower layer of cubes and horizontally into the upper layer of cubes. In the lower layer, the grids are arranged within the rig to form concentric squares around the centre cube. 4 or 7 concentric squares of grids can be used around the central cube. The bars of each grid were in line with the bars on the other grids and the grids are spaced at 0.15 m apart. The first vertical grid was at 0.57 m from the ignition point for the 4 and 7 grid systems. The last grid was at 1.0 m from the ignition point for the 4-grids system and 1.43 m for the 7 grids system. In the top layer, the grids were placed horizontally of same dimensions. Each grid ran the full length of the frame of 3 m and was of one cell width of 1 m. For the 4 and 7 layers of grids, alternating layers running left to right and front to back were used in the experiments as shown in Figure 1. The first horizontal grid is at 0.57 m from the ignition point and the last grid was 1.43 m. The ignition location is at the centre of the bottom central cube. The overpressures are measured by using two type of sensors: Hydrophones (H) and Kulite (K) type, hydrophones were used to record 'lower' overpressures and Kulite piezo-resistive transducers were used to measure the 'higher' overpressures. Hydrophones had a measurement error of ± 0.5 kPa and the Kulite sensors ± 0.8 kPa. The hydrophones were mounted in poles and the piezo-resistive sensors were mounted in streamlined blocks fixed into a short length of scaffolding fixed to the ground. The lines of the sensors for the 4 and 7-gate experiments shown in Figure 2. The red and black concentric lines in the Figure 2 are representative of 7 and 4-gate configurations grid placement in the lower cube layers.

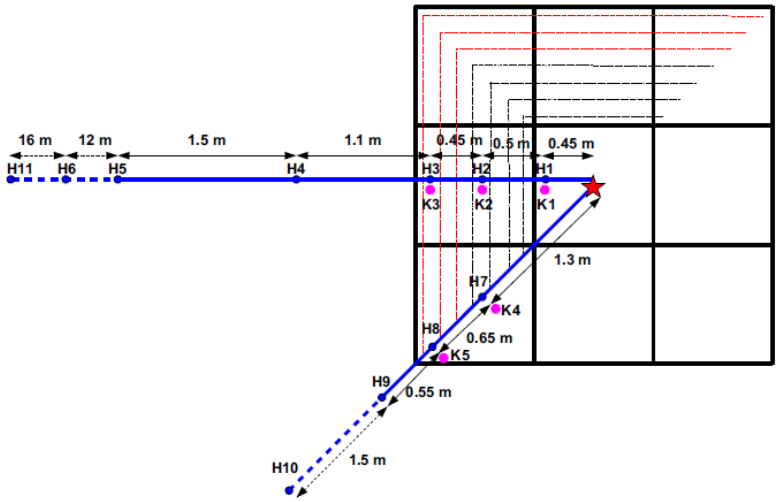

Figure 2. Overpressure sensor location w.r.t centre of the pipe rig in top view.

Table 1. Overpressure sensor locations.

S.no	Sensor	Angle	Horizontal distance from spark (m)	Height above ground (m)
1	H1	180	0.45	0.5
2	K1	180	0.45	0.5
3	H2	180	0.95	0.5
4	K2	180	0.95	0.5
5	H3	180	1.4	0.5
6	K3	180	1.4	0.5
7	H4	180	2.5	0.5
8	H5	180	4	0.5
9	H6	180	16	1.2
10	H11	180	32	0.5
11	H7	135	1.3	0.5
12	K4	135	1.3	0.5
13	H8	135	1.95	0.5
14	K5	135	1.95	0.5
15	H9	135	2.5	0.5

The exact location of the overpressure sensors is tabulated in Table 1, distances are w.r.t the ignition (spark) location. The pipe rig was covered with clinging plastic sheet to retain the flammable gas mixture. The plastic film was cut at the corners prior to ignition to limit the confinement presented by the film on the ignition. The hydrogen experimental tests conditions considered in the present study for CFD results validation are presented in Table 2. Also 4 and 7-gate test configuration are considered for numerical investigation. The contained gas volume and the volume blockage ratio for the 4-gates (with Kulite stands) are 17.487 and 2.85 respectively, and for 7-gates (with Kulite stands) are 17.230 and 4.28 respectively.

Table 2. Test conditions for hydrogen-air pipe rig experiments.

S.no	Parameters	Experiment Hydrogen06	Experiment Hydrogen07	Experiment Hydrogen15	Experiment Hydrogen16
1	Number of gates	4	4	4	7
2	Free volume (m^3)	17.49	17.49	17.487	17.23
3	Gas mixture temperature	35.2	39.3	15.6	23.9
4	Ratio of hydrogen to oxygen	1.937	1.933	2.507	2.334
5	Stoichiometric ratio of mixture	0.969	0.967	1.253	1.167
6	Mass of hydrogen ignited (kg)	0.422	0.417	0.524	0.481

4.0 NUMERICAL SETUP

The computational geometry for the two configurations of 4 & 7-gates are shown Figure 3 (x-y plane is the ground level and the z-direction is the elevation). The dimensions of the simulation domain enclosing the pipe rig are chosen such that the effects of end boundary condition were minimal on the predictions at the monitoring locations close to the rig as given in Table 1. The computational domain dimensions are 40 m x 40 m x 15 m to also enable the pressure sensor measurements at 16 m from the pipe rig in the numerical simulations.

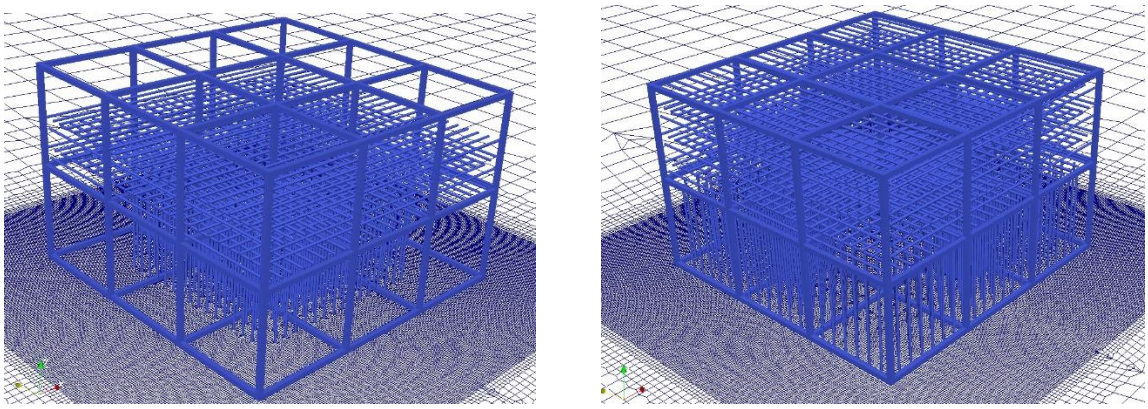

Figure 3. Computational geometry for the 4 & 7-gate pipe rig configuration.

The CFD domain is discretized into nonuniform hexahedron dominant mesh, the cell size varied from 5 mm at the ignition location to 0.5 m at the open boundary. The mesh distribution in horizontal and vertical planes are shown in Figure 4. The mesh is generated using OpenFOAM mesh utilities.

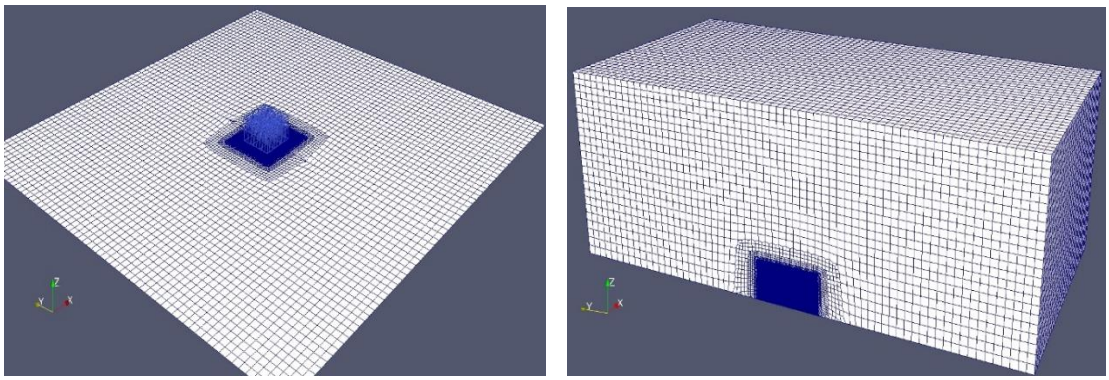

Figure 2. Mesh distribution around the pipe rig

The premixed near stoichiometric hydrogen-air cloud is initialized using 'setField' utility in OpenFOAM (further details are available in [13]). The ambient conditions are taken as 1 atm pressure with no wind conditions. The locations of the monitoring points (pressure sensors) considered for the overpressure measurements in numerical study are upto 16 m distance from the rig center (listed in Table 1). Ignition of the premixed cloud is initiated with a hot patch initialized with burnt product composition and temperature. The mesh refinement at the ignition location and tuning of the ignition parameters such as the ignition patch volume, ignition burnt mass fraction are parametrized to better match well the initial pressure rise and first peak overpressure for the validation cases and then left unaltered for the remaining CFD prediction cases.

Table 3. Numerical simulation conditions for hydrogen-air pipe rig.

S.no	Parameters	Numerical Hydrogen04	Numerical Hydrogen05	Numerical Hydrogen06	Numerical Hydrogen07	Numerical Hydrogen15	Numerical Hydrogen16
1	Number of gates	4	7	4	7	4	7
2	Gas mixture temperature	35.2	35.2	35.2	39.3	15.6	23.9
3	Stoichiometric ratio of mixture	0.5	0.5	0.969	0.967	1.253	1.167
4	Mass of hydrogen ignited (kg)	0.31	0.31	0.422	0.417	0.524	0.481

The numerical simulation conditions are listed in Table 3. The simulation cases 'Hydrogen15' and 'Hydrogen16' are run for CFD prediction validations. The remaining cases 'Hydrogen04, Hydrogen05, Hydrogen06, Hydrogen07' are run for making CFD predicting of overpressure trends for change in congestion and the mixture composition. No-slip and adiabatic boundary condition are imposed on the wall surfaces. Improper treatment of pressure and velocity at outlet boundary in simulations can lead to spurious numerical wave reflections that can seriously affect the solution. A partial non-reflective pressure boundary condition implemented in OpenFOAM named as 'waveTransmissive' is applied to pressure and 'zeroGradient' condition is applied for the velocity at the domain enclosure surface (outlet).

5.0 RESULTS AND DISCUSSION

The pressure trace curves for 4 & 7-gate configuration at 2.5 m and 16 m probe location are shown in Figure 3 & 4, along with the experimental results. The experimental pressure curves are digitized from the reference [1]. The probe locations 2.5 m and the 16 m lies in the coarse mesh region of the computational domain, hence the pressure trace seems to be more oscillatory than the experimental results, also the oscillations present in the numerical predictions after the peak curve are having contributions of the partial reflections from the end boundary.

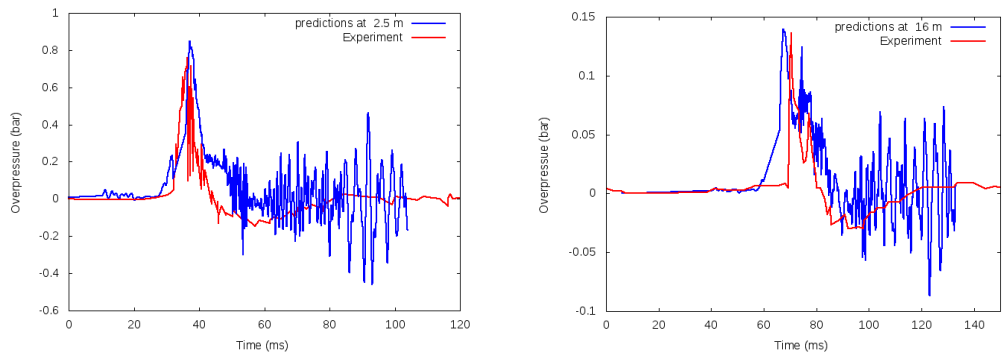

Figure 3. Overpressure trace curve at the probe location 2.5 m and 16 m for 4-gate experiment (Hydrogen15).

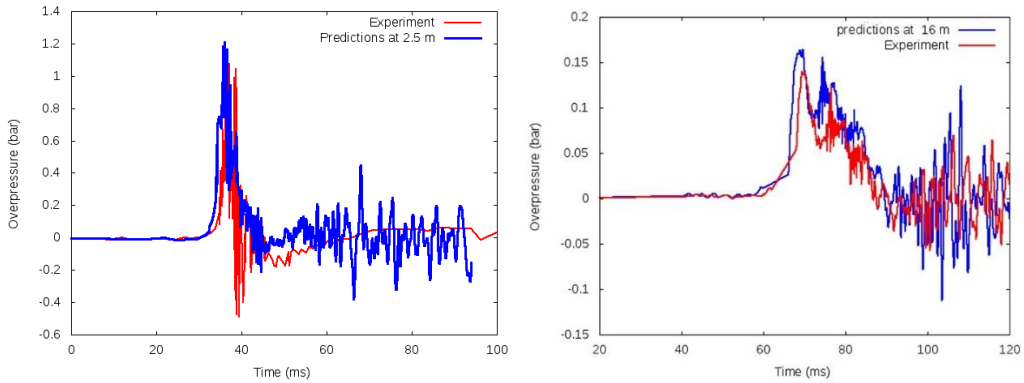

Figure 4. Overpressure trace curve at the probe location 2.5 m and 16 m for 7-gate experiment (Hydrogen16).

The numerical predictions are time averaged for 5 ms to smoothen the overpressure trace curves. The overpressure values at the probe location 2.5 m and 16 m are tabulated in Table 4, for simulation cases considered on this present work. The ignition parameters such as the ignition patch volume, ignition burnt mass fraction are initially adjusted to match well with the initial pressure rise for the validation

cases and then these values are left unaltered for the remaining CFD prediction cases. The mesh at the ignition location was refined so that the cell size is close to 5 mm based on author previous work [11].

Table 4. Summary of the overpressure magnitudes for tests listed in Table 3.

S.0	Test	No. of gates	laminar flame speed (m/s)	Equivalence ratio	Experiments overpressure (bar)		Predicted overpressure (bar)	
					at 2.5 m	at 16 m	at 2.5 m	at 16 m
1	Hydrogen16	7	2.38	1.167	1.17	0.148	1.21	0.172
2	Hydrogen15	4	2.52	1.253	0.72	0.145	0.822	0.148
3	hydrogen07	7	1.89	0.967	-	-	0.931	0.233
4	Hydrogen06	4	1.89	0.969	0.48	0.152	0.61	0.186
5	Hydrogen05	7	0.45	0.5	-	-	0.356	0.083
6	Hydrogen04	4	0.45	0.5	-	-	0.282	0.052

From the overall results it is discernible that the congestion is playing a much dominant role on the overpressure magnitudes. Mixture with same reactively (with Hydrogen04 & Hydrogen05) surely higher congestion produces higher overpressures. Even for the mixtures with lower reactivity (between Hydrogen16 & Hydrogen15) produced the higher overpressure magnitudes due to higher congestion. Consistent trends are predicted for the overpressures for the test cases Hydrogen07, Hydrogen06, Hydrogen05 and Hydrogen04, higher congestion produced higher overpressure. The mixture reactivity is assessed by hydrogen-air mixtures unstretched laminar flame speed values, computed using the correlation of [16]. The role played by the congestion in the flame propagation can be interpreted in terms of the flame surface generated during the flame-obstacle interactions. Figure 5, shows are flame front contours at two instance of time during the flame propagation, while interacting with pipe rig congestion. It can be seen for the flame instantaneous contours that the flame propagation velocities are slightly higher in the central region compared to the corners of the pipe rig. These variations in the flame

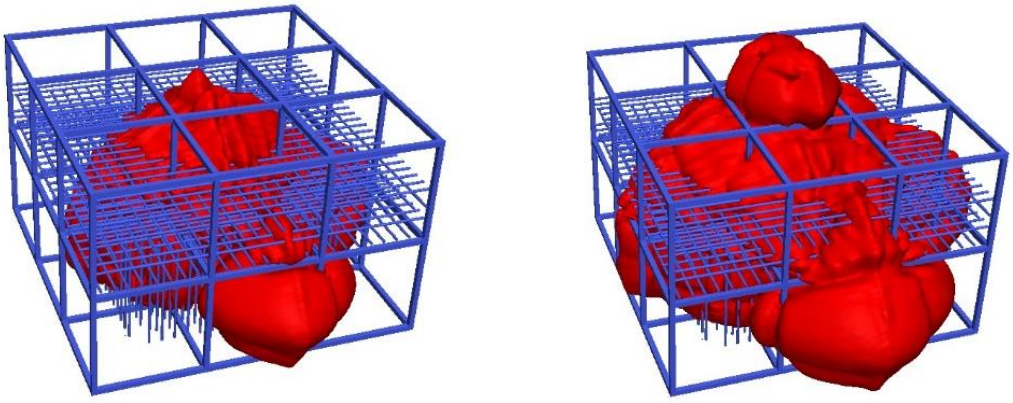

Figure 5. Flame front contour at some instant of time propagation.

propagation velocities along and the diagonal and the central axis of the pipe rig are also reflected in the differences in overpressure magnitudes measured along the two sensor lines (Figure 2) [1].

6.0 CONCLUSIONS

The flame surface wrinkling model is employed to model the turbulent flame deflagrations. The turbulent flame speed correlation is considered with Lewis no. factor. Overall, six scenarios are studied involving a change in number of gates and the hydrogen concentration. The simulation predictions for one each of the 4 & 7-gate case are compared with experiments. The ignition parameters such as the ignition patch volume, ignition burnt mass fraction are initially adjusted to match well with the initial pressure rise for the validation cases and then these values are left unaltered for the remaining CFD prediction cases. The results demonstrated that the congestion is dominant factor in generation of the deflagration overpressures. Even for the mixtures with lower reactivity (between Hydrogen16 & Hydrogen15) produced the higher overpressure magnitudes due to higher congestion. The comparisons between model predictions and experimental data presented in this paper show that a CFD explosion model can provide reasonable predictions of the overpressures developed during hydrogen/air deflagrations, once the simulation parameters are well adjusted for the given mesh resolutions. Thus, such models can be used with reasonable confidence to explore geometries of practical applications beyond those tested in experiments and examine mitigating consequences in the unlikely event of accidental hydrogen leakage, ignition, and explosion. The study has demonstrated the potential of the open source code to be used as a predictive tool to aid facility siting and mitigation measures for improved safety of hydrogen installations.

REFERENCES

1. Shirvill, L. C., Roberts, T. A., Royle, M., Willoughby, D. B., Sathiah, P., Experimental study of hydrogen explosion in repeated pipe congestion – Part 1: Effects of increase in congestion, International Journal of Hydrogen Energy, 2018. 1-18.
2. Weller, H. G., Tabor, G., Gosman, A. D., and Fureby, C., Application of a flame wrinkling LES combustion model to a turbulent mixing layer (1998), Proc. of Combust. Inst., 27.
3. Shirvill L. C., Roberts T. A., Royle M., Willoughby D. B., Gautier T., Safety studies on high-pressure hydrogen vehicle refuelling stations: releases into a simulated high-pressure dispensing area. Int J Hydrogen Energy 2011; 37 (2012):6949-64.
4. Shirvill L. C., Roberts T. A., Royle M, Willoughby D. B., Sathiah P., Effects of congestion and confining walls on turbulent deflagrations in a hydrogen storage Facility-Part 1: Experimental Study. Int J Hydrogen Energy 2018;43(15):7618-42.
5. Makarov D., Verbecke F., Molkov V, Roe O., Skotenne M., Kotchourko A., et al. An inter-comparison exercise on CFD model capabilities to predict a hydrogen explosion in a simulated vehicle refuelling environment. International Journal of Hydrogen Energy 2009;34(6):2800–14
6. Kikukawa S., Consequence analysis and safety verification of hydrogen fuelling stations using CFD simulation. International Journal of Hydrogen Energy 2008;33(4):1425–34.
7. Baraldi D, Venetsanos A. G., Papanikolaou E., Heitsch M., Dallas V., Numerical analysis of release, dispersion and combustion of liquid hydrogen in a mock-up hydrogen refuelling station. Journal of Loss Prevention in the Process Industries 2009;22(3):303–15.
8. Tchouvelev A.V., Cheng Z, Agranat V. M., Zhubrin S. V., Effectiveness of small barriers as means to reduce clearance distances. International Journal of Hydrogen Energy 2007; 32(10–11):1409–15.
9. Papanikolaou E. A, Venetsanos A. G., CFD simulations of hydrogen release and dispersion inside the storage room of a hydrogen refuelling station using the ADREA-HF code. In: Proc. 2nd International conference on hydrogen safety. Spain; Sept. 11–13. 2007
10. Wen J. X., Madhav Rao V. C., Tam V. H. Y., Numerical study of hydrogen explosions in a refuelling environment and in a model storage room. Int. J Hydrogen Energy 2010; 35:385-94.
11. Madhav Rao V. C., Wen J. X., Sathiah P. Effects of congestion and confining walls on turbulent deflagrations in a hydrogen storage Facility-Part 2: numerical study. Accepted for publication in Int J. Hydrogen Energy, 2018, Volume 43, Issue 32 :15593-15621.

12. Fureby C., Gavin, T., Weller H. G., Gosman A.D., A comparative study of subgrid scale models in homogeneous isotropic turbulence. Phys Fluids 1997; 9:1416-29.
13. Weller H. G., Gavin, T., Gosman A. D., Fureby C., Application of a flame-wrinkling les combustion model to a turbulent mixing layer. Symp. Int. Combust 1998;27(1):899-907.
14. Tabor G, Weller HG. Large eddy simulation of premixed turbulent combustion using Xi-flame surface wrinkling model, Flow Turbul. Combust. 2004;72(1):1-27.
15. Bradley D., Lau A. K. C., Lawes M., Flame stretch as a determinant of turbulent burning velocity. Philosophical Transactions of the Royal Society of London, Series A: Mathematical and Physical Sciences, 338:359-387, 1992
16. Ravi, S., Petersen, E. L., Laminar flame speed correlations for pure-hydrogen and high-hydrogen content syngas blends with various diluents, International Journal of Hydrogen Energy 37 (24), 19177-19189